Neurobiology of Disease

Altered Intracellular Ca^{2+} Homeostasis in Nerve Terminals of Severe Spinal Muscular Atrophy Mice

Rocío Ruiz, Juan José Casañas, Laura Torres-Benito, Raquel Cano, and Lucía Tabares
Department of Medical Physiology and Biophysics, School of Medicine, University of Seville, 41009 Seville, Spain

Low levels of survival motor neuron (SMN) protein result in spinal muscular atrophy (SMA), a severe genetic disease characterized by motor impairment and premature lethality. Although SMN is a ubiquitous protein, motor neurons are much more vulnerable to low levels of SMN than other cells. To gain insight into the pathogenesis of SMA, we have compared synaptic function of motor terminals in wild-type and severe SMA mice at different ages and in two proximal muscles. Our results show that mutant muscle fibers fire normal action potentials and that multi-innervated terminals are functional. By studying the characteristics of the three main components of synaptic transmission in nerve terminals (spontaneous, evoked, and asynchronous release), we found that the kinetics of the postsynaptic potentials are slowed and evoked neurotransmitter release is decreased by ~55%. In addition, asynchronous release is increased ~300%, indicating an anomalous augmentation of intraterminal bulk Ca^{2+} during repetitive stimulation. Together, these results show that the reduction of SMN affects synaptic maturation, evoked release, and regulation of intraterminal Ca^{2+} levels.

Introduction

Spinal muscular atrophy (SMA), the leading genetic cause of infant mortality (Crawford and Pardo, 1996), is an autosomal recessive degenerative disease of lower motor neurons. Symptoms include muscular weakness and atrophy of limb and trunk muscles. SMA is caused by mutations or loss of the *SMN1* gene and retention of the *SMN2* gene (Lefebvre et al., 1995); both genes encode for the survival motor neuron (SMN) protein. The best-characterized SMN function is its participation in the assembly of small nuclear ribonucleoproteins (Fischer et al., 1997; Liu et al., 1997; Meister et al., 2001; Pellizzoni et al., 2002). In the absence of a functional *SMN1* gene, the severity of the disease depends on the amount of full-length SMN (SMN-FL) produced by *SMN2*. The majority of transcripts from the *SMN2* gene lack exon 7 (SMNΔ7), but a small amount of the transcript is SMN-FL (Gennarelli et al., 1995; Lorson et al., 1999; Monani et al., 1999). Although SMN is a ubiquitous protein, deficient levels of SMN predominantly damage lower motor neurons (Monani et al., 2000). It has been proposed that SMA is a motor neuron "dying back" axonopathy, supported by the finding that in SMA there is substantial accumulation of neurofilaments in terminal axons followed by a major loss of motor neurons (Cifuentes-Diaz et al., 2002; Kariya et al., 2008). It has also been postulated that the reduction of SMN produces a motor neuron synaptopathy manifested by the arrest of the postnatal development of the neuromuscular junction (NMJ) and a functional deficit (Kariya et al., 2008; Kong et al., 2009). Electrophysiological analysis in the tibialis anterior (TA) muscle of a relatively severe SMA mouse model (Le et al., 2005; Butchbach et al., 2007; Murray et al., 2008; Kong et al., 2009) shows that the number of synaptic vesicles that release neurotransmitter during an action potential is decreased (Kong et al., 2009).

We sought to address the cellular mechanism of the pathogenesis of SMA by studying further the electrophysiological properties of neuromuscular synaptic transmission in the SMNΔ7 SMA mouse mutant. We have studied two proximal muscles, a pure fast-twitch muscle [Levator auris longus (LAL), located at the dorsal surface of the head and innervated by the facial nerve] and a predominantly slow twitch muscle [Transversus abdominis (TVA), a postural muscle from the anterior abdominal wall innervated by lower intercostal nerves]. We examined neuromuscular transmission at two stages, at an early age [postnatal days 7–8 (P7–8)], where the motor dysfunction is already evident (Le et al., 2005), and at a later age (P14–15), coincident with the end of the mouse life period. We hypothesized that in SMA there is an early synaptic dysfunction in motor nerve terminals. We first studied the ability of mutant muscular fibers to trigger action potentials upon stimulation from the presynaptic terminal. Next, we investigated the functionality of multiple nerve terminals innervating the same myofiber.

Finally, we investigated the capacity of presynaptic terminals to release neurotransmitters in three modes: (1) at rest (spontaneous release), (2) upon a single action potential (synchronous evoked release), and (3) during intraterminal Ca^{2+} accumulation resulting from prolonged electrical stimulation (asynchronous release). In SMA we found that in addition to severe evoked neurotransmission defects, there was an abnormal increase in the amount of Ca^{2+}-dependent asynchronous release during prolonged stimulations, suggesting an altered intraterminal bulk Ca^{2+} concentration in SMA synapses.

Received Sept. 9, 2009; revised Oct. 11, 2009; accepted Nov. 23, 2009.

This work was supported by grants from GENAME and the Spanish Ministry of Education and Science, BFU2007-61171 and BES2005-6739. We are grateful to Drs. Guillermo Alvarez de Toledo and Manel Santafé for helpful comments.

Correspondence should be addressed to Lucía Tabares, Department of Medical Physiology and Biophysics, School of Medicine, University of Seville, Avenida Sánchez Pizjuan, 4, 41009 Seville, Spain. E-mail: ltabares@us.es.

DOI:10.1523/JNEUROSCI.4496-09.2010

 0270-6474/10/300849-09$15.00/0

Materials and Methods

Animal model. Mouse lines were kindly provided by Dr. A. Burghes (Department of Molecular Genetics, College of Biological Sciences, The Ohio State University, Columbus, OH). Experimental mice were obtained by breeding pairs of SMA carrier mice ($Smn^{+/-}$;$SMN2^{+/+}$;$SMN\Delta7^{+/+}$) on a FVB/N background. Identification of wild-type (WT) and mutant mice ($Smn^{-/-}$;SMN2;SMNΔ7) was done by PCR genotyping of tail DNA as previously described (Le et al., 2005). All WT mice used were age-matched littermates of mutants. All experiments were performed according to the guidelines of the European Council Directive for the Care of Laboratory Animals.

Muscle preparation. Mice were anesthetized with tribromoethanol (2%, 0.15 ml/10 g body weight, i.p.) and killed by exsanguination. The LAL and TVA muscles were dissected with their nerve branches intact and pinned to the bottom of a 2 ml chamber, over a bed of cured silicone rubber (Sylgard, Dow Corning). Preparations were continuously perfused with a solution of the following composition (in mM): 125 NaCl, 5 KCl, 2 $CaCl_2$, 1 $MgCl_2$, 25 $NaHCO_3$ and 15 glucose. The solution was continuously gassed with 95% O_2 and 5% CO_2, which maintained the pH at 7.35. Recording was performed at room temperature (22−23°C).

Ex vivo *electrical stimulation and intracellular recording.* The nerve was stimulated by means of a suction electrode. The stimulation consisted of square-wave pulses of 0.2–0.5 ms duration and 2–40 V amplitude, at variable frequencies (0.5–20 Hz). A glass microelectrode (10–20 MΩ) filled with 3 M KCl was connected to an intracellular recording amplifier (Neuro Data IR283; Cygnus Technology) and used to impale single muscle fibers near the motor nerve endings. Evoked endplate potentials (EPPs) and miniature EPPs (mEPPs) were recorded from different NMJs within the muscle as described previously (Ruiz et al., 2008). Muscular contraction was prevented by including in the bath 3–4 μM μ-conotoxin GIIIB (Alomone Laboratories), a specific blocker of muscular voltage gated sodium channels. In a number of experiments 10 or 100 μM EGTA-AM (Calbiochem) was added to the chamber; after 30 min of incubation the solution was exchanged with a solution without EGTA.

Data analysis. The mean amplitudes of the EPP and mEPPs recorded at each NMJ were linearly normalized to −70 mV resting membrane potential. EPP amplitudes were corrected for nonlinear summation (Martin, 1955) as follows: EPPc = Average Peak EPP/(1 − Average Peak EPP/($V_m - E_r$)), where V_m is the resting membrane potential and E_r the reverse potential (assumed to be −5 mV for all of our experiments). The kinetics of EPP and mEPP were characterized by their rise time (10–90%) and decay time constant (calculated from the exponential fit of the decay phase). Quantal content (QC) was estimated by the direct method, which consists of recording mEPPs and EPPs (nerve stimulation 0.5 Hz) simultaneously and then calculating the ratio: QC = Average Peak EPP/Average Peak mEPP. The rate of asynchronous release during the train was estimated by counting mEPPs occurring during the interstimulus interval, after the EPP had decayed to near-baseline levels. All electrophysiological data are given as group mean values ± SEM, unless otherwise stated, with *n* being the number of muscles fibers per group and *N* the number of mice per group. All experiments reported include the results of at least three animals per genotype. Statistical comparisons between mutant and wild-type measures were made using Student's *t* test (two-tailed unless otherwise stated) when the distribution was normal and Mann–Whitney rank sum test when the distribution was not normal. Results were considered statistically different when the *P* value was <0.05.

Immunohistochemistry. Dissected muscles were fixed in 4% paraformaldehyde. Muscles were bathed with 0.1 M glycine in PBS for 20 min, then permeabilized with 1% (v/v) Triton X-100 in PBS for 30 min, and incubated then in 5% (w/v) BSA, 1% Triton X-100 in PBS for 2 h. Samples were incubated overnight at 4°C with primary antibody against 160 kDa neurofilament (NF) (1:750, Millipore). Next day muscles were rinsed for 1 h in PBS containing 1% Triton X-100, incubated for 1 h both with 4 μg/ml Alexa 488-conjugated goat anti-mouse secondary antibody (Invitrogen) and 10 ng/ml rhodamine-BTX and rinsed again with PBS for 90 min. Finally, muscles were mounted in glycerol containing DABCO and imaged with an upright Olympus FV1000 confocal microscope. Z-stack projections were made from serial scanning every 0.5 μm to reconstruct the NMJ.

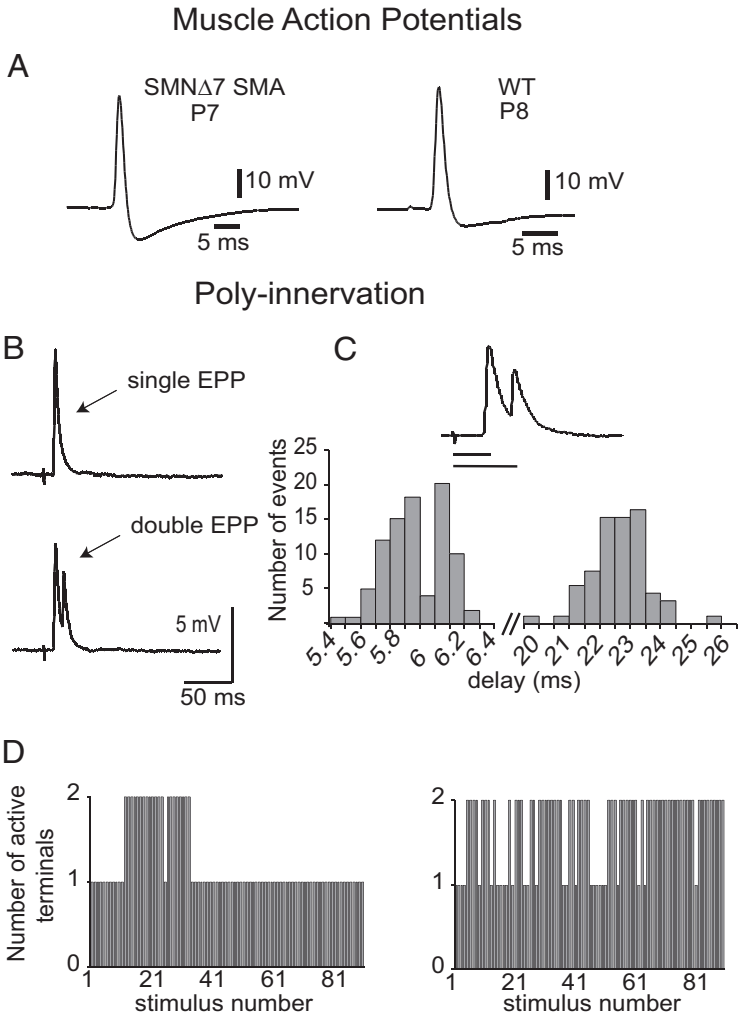

Figure 1. Muscle action potentials and poly-innervation in SMNΔ7 SMA mutant mice. ***A***, Representative traces of action potentials recorded in a SMA and wild-type mice in the LAL muscle, at P7–8. ***B***, Example of EPPs recorded after single nerve stimulation in a mono-innervated fiber (upper trace) and in a double innervated fiber (bottom trace). ***C***, Frequency distribution of delays between the stimulation artifact and the EPP peaks. The inset shows an example of delay measurements (horizontal lines). ***D***, Representation of the number of active nerve terminals per stimulation in two mutant fibers.

Results

Normal muscular action potential in mutant SMNΔ7 SMA mice

SMNΔ7 SMA mice show a severe phenotype within the first 2 weeks of life, characterized by low body weight, decreased mus-

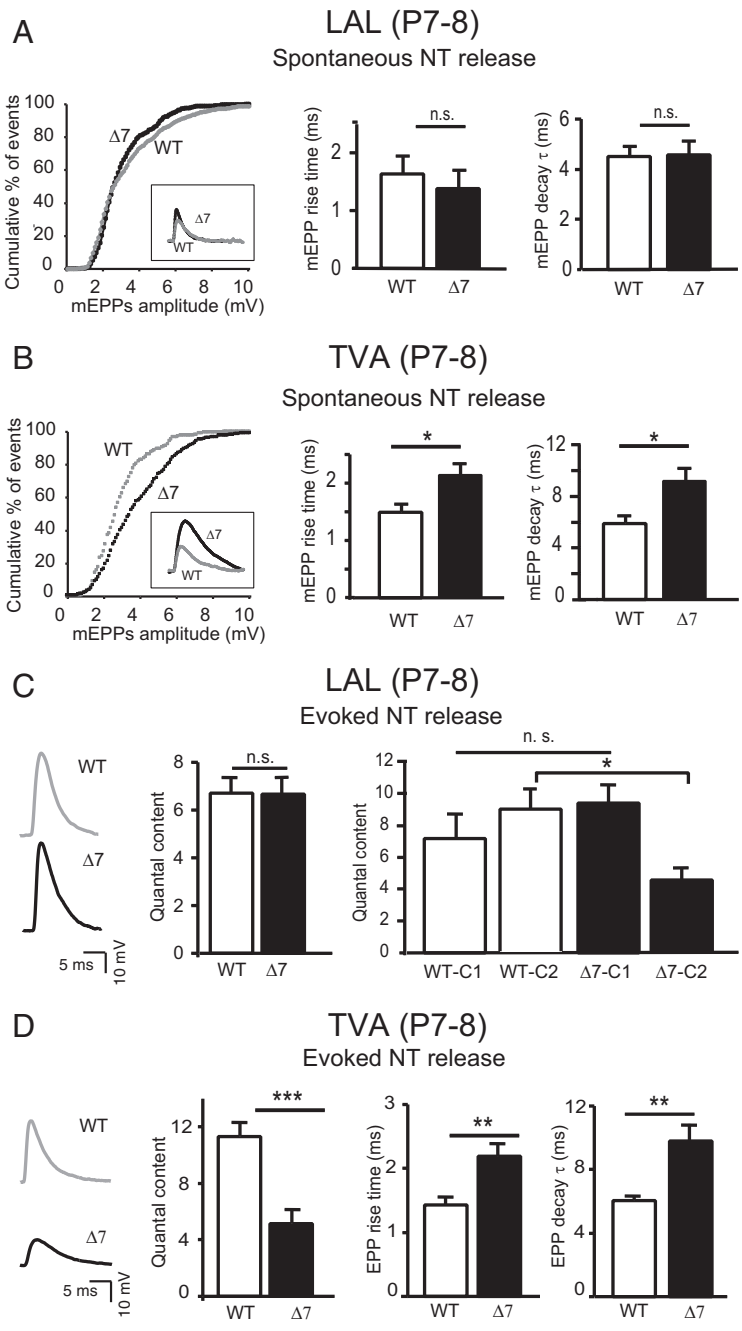

Figure 2. Spontaneous and evoked neurotransmitter release properties in LAL and TVA muscles at P7–8. ***A***, Cumulative frequency of mEPP amplitudes (WT: gray curve, *n, N* = 14, 4; mutant: black curve, *n, N* = 10, 4); mEPP rise and decay times (WT: *n, N* = 7, 3; mutant: *n, N* = 6, 3) in LAL muscle. ***B***, Cumulative frequency of mEPP amplitudes (WT: gray curve, *n, N* = 14, 3; mutant: black curve, *n, N* = 18, 3); mEPP rise and decay times (WT: *n, N* = 13, 3; mutant: *n, N* = 14, 3) in TVA muscles. Insets in left panels (***A*** and ***B***) are averaged mEPPs from WT (gray traces, *n* = 20) and mutant (black traces, *n* = 20) muscle fibers (same scale for all four traces). ***C***, Representative EPP traces, total QC (WT, *n, N* = 32, 9; mutant, *n, N* = 34, 9), and caudal QC after segregating the data into the two caudal regions (***C1*** and ***C2***), (WT ***C1***: *n, N* = 10, 2; ***C2***: *n, N* = 8, 3; mutants ***C1***: *n, N* = 7, 4; ***C2***: *n, N* = 16, 3). ***D***, Representative EPP traces, QC (WT: *n, N* = 14, 3; mutant: *n, N* = 19, 3) and EPP rise and decay times (WT: *n, N* = 13, 3; mutant: *n, N* = 16, 3). **p* < 0.05, ***p* < 0.005, ****p* < 0.0005. n.s., No significance.

cular strength, and low motor motility, which quickly result in early lethality (Le et al., 2005; Butchbach et al., 2007; Murray et al., 2008; Kong et al., 2009).

We have performed intracellular recordings to study neurotransmission and muscular electrical excitability of SMNΔ7 SMA mice and wild-type littermates in two proximal muscles LAL and TVA, from P7–15. In these two muscle types, muscular fibers from mutant or wild-type mice were able to contract in response to electrical nerve stimulation, and contractions were efficiently blocked by the same amount of μ-conotoxin (3–4 μM)—a specific blocker of muscular Na^+ channels. We also found that muscle action potentials (APs) were normal in SMA mice when the amplitude of the EPP reached threshold (Fig. 1*A*). The analysis of muscle AP showed the expected characteristics (peak amplitude, duration, and posthyperpolarization size) in both wild-type and mutant mice at both P7 and P14, demonstrating that muscle fibers were initially innervated and able to generate normal APs.

Poly-innervation in SMNΔ7 SMA mice is functional

Poly-innervation is a normal feature of mouse muscular fibers during the first 2 weeks of life (Sanes and Lichtman, 1999). In SMA mutant mice, it has been shown that the number of axons innervating single muscular fibers is not different from wild-type littermates (Kariya et al., 2008). To test the functionality of the different nerve terminals reaching an individual muscular fiber in SMNΔ7 SMA mice, we recorded the number of evoked potentials elicited by single nerve stimuli of different strengths.

In mutants, as in wild-type littermates, low strength nerve stimulation (2–5 V) produced a single evoked end-plate potential (Fig. 1*B*, upper trace), but more complex signals (usually double peak responses, Fig. 1*B*, lower trace) when the stimulus strength was increased (>10 V), indicating the activation of different threshold nerve terminals over the same muscle fiber (Redfern, 1970; Colman et al., 1997; Santafé et al., 2001). In the double responses, the peaks were easily distinguishable due to their different timings. We then measured the delays between the stimulus artifact and each peak (see example trace in Fig. 1*C*). Usually, the representation of the delay values from a given muscular fiber showed two clear distributions, whose relative area represented the synaptic activity of each synaptic input (Fig. 1*C*).

In most recordings, the terminals with the shorter delay were more active (they responded to the stimulus at almost all times) than those with the longer delay. However, in some cases, both terminals were almost equally active; examples are shown in Figure 1, *C* and *D* (right graph). No specific temporal pattern in the synaptic activity of the less active terminal was found. During loss of polysynaptic innervation the active terminal will be retained which is equivalent to the synapse with the short delay.

The strength of the inputs innervating the same muscle fiber were also typically different, as shown in the traces in Figure 1, *B* and *C*, with the stronger response usually being followed by the weaker one, which is another indication that the muscular fibers were already undergoing a switch from multiple to single axonal innervation (Colman et al., 1997). We found an increased number of SMNΔ7 SMA muscular fibers with single EPP responses in P13–14 mice (data not shown), suggesting that they had already achieved single axonal innervation. These results demonstrate the functionality of multiple motor nerve inputs contacting a single muscular fiber during the early postnatal age of SMNΔ7 SMA mice and confirm previous observations (Murray et al., 2008) that the reduction of SMN levels in mice do not interfere with the formation of multiple synapses in the same muscular fiber.

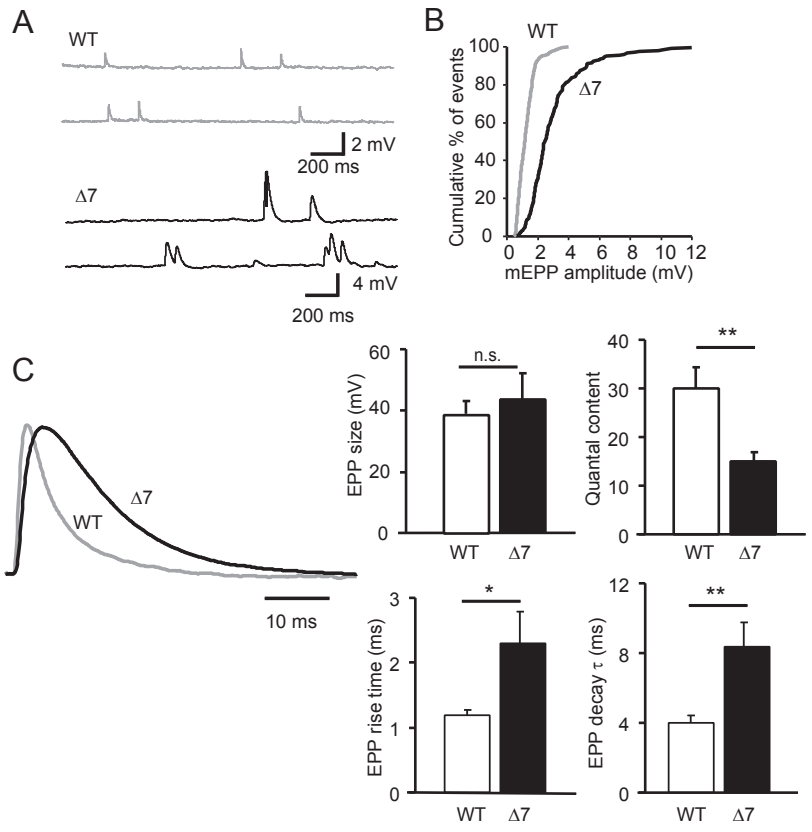

Figure 3. Spontaneous and evoked neurotransmitter release in TVA muscles in mutant terminals at P14–15. ***A***, Representative recording of mEPPs in wild-type (gray trace) and mutant (black trace) terminals. ***B***, Cumulative frequency of mEPP amplitudes in WT (gray curve, *n*, $N = 20, 4$) and mutant (*n*, $N = 19, 5$). ***C***, Amplitude normalized representative EPP's traces in WT (gray line) and mutant (black line) fibers. Upper graphs, EPP size and QC in wild-type and mutant terminal (*n*, $N = 20, 4$; *n*, $N = 19, 5$, respectively). Lower graphs, Kinetic of EPPs in wild-type (*n*, $N = 19, 4$) and mutant terminals (*n*, $N = 17, 5$). $*p < 0.05$, $**p < 0.005$. n.s, No significance.

Spontaneous neurotransmitter release is preserved in the LAL but not in the TVA muscles during early postnatal life

To investigate the effect of SMN deficiency on spontaneous neurotransmitter release (independent of action potentials) during early postnatal life (P7–P9), we compared different characteristics of the mEPPs in two muscles (LAL and TVA) from wild-type and mutant mice.

First of all, we analyzed the amplitudes of mEPPs from wild-type and mutant terminals. In LAL muscles, the median mEPPs amplitude in mutant fibers (2.52 mV) was not statistically different from that of wild-types (2.55 mV), as determined by the cumulative frequency distribution of mEPPs (Fig. 2*A*). However, in TVA muscles, the distribution curve in mutants shifted to the right (Fig. 2*B*), with the mEPPs median amplitude being significantly larger ($p < 0.001$; Mann–Whitney test) in mutants (3.45 mV) than in wild-types (2.63 mV). This difference was probably due to the smaller size of mutant myofibers in this muscle, which resulted in a higher input resistance and, consequently, a greater voltage change. This data excludes the possibility of SMA synapses having a reduced sensitivity of the postsynaptic receptors to ACh, or a decrease in the amount of transmitter contained in synaptic vesicles.

Next, we compared the frequency of spontaneous neurotransmitter release and found that, although it varied greatly between terminals in mutant mice, there was no statistical differences between wild-type (6.44 ± 1.8; *n*, $N = 34, 10$) and mutant (13.93 ± 4; *n*, $N = 26, 9$) LAL terminals ($p = 0.1$). However, in the TVA muscle, the frequency mEPPs was significantly greater in mutant terminals (mutants: 14.39 ± 3.5; *n*, $N = 18, 3$; wild-types: 4.22 ± 0.82; *n*, $N = 14, 3$; $p < 0.014$).

Finally, we compared the kinetics (rising and decay time) of mEPPs from mutant and wild-type terminals from the two muscles. No differences were found between wild-type and mutant terminals in the LAL (Fig. 2*A*) while in the TVA, the rise time and the decay time constant of mEPPs were prolonged (Fig. 2*B*), suggesting a delay in the maturation of the postsynaptic receptors. All together, these results show that at 1 week of age, the spontaneous neurotransmitter release in mutants was not significantly affected in the LAL while it was already modified in the TVA muscles.

Early and selective impairment of evoked neurotransmitter release

We examined whether the deficiency in SMN affects the amount of evoked neurotransmitter release at motor terminals in response to a single action potential [quantal content (QC)], at P7-P8, in the two muscles under study (LAL and TVA). In LAL, the mean size of the EPPs in SMA animals was larger than in wild-types (mutants: 57.4 ± 11.4; wild types: 42.3 ± 5.12), but the difference did not reach statistical significance ($p = 0.1$). We also compared QC values of mutants and wild-types and found no difference either ($p = 0.99$) (Fig. 2*C*, left graph). However, morphological analysis has previously shown that the caudal branches innervating this muscle are selectively vulnerable in mutant SMA mice (Murray et al., 2008). To address this point we compared the QC in the caudal and rostral muscle bands and found no differences between mutants and wild-type terminals ($p = 0.22$). Nevertheless, when we divided QC values from the caudal band into its two anatomical components, C1 (lateral) and C2 (medial), we found an almost twofold reduction of QC in C2 in mutants (4.46 ± 0.7) in comparison with wild type (8.79 ± 1.3; $p <$

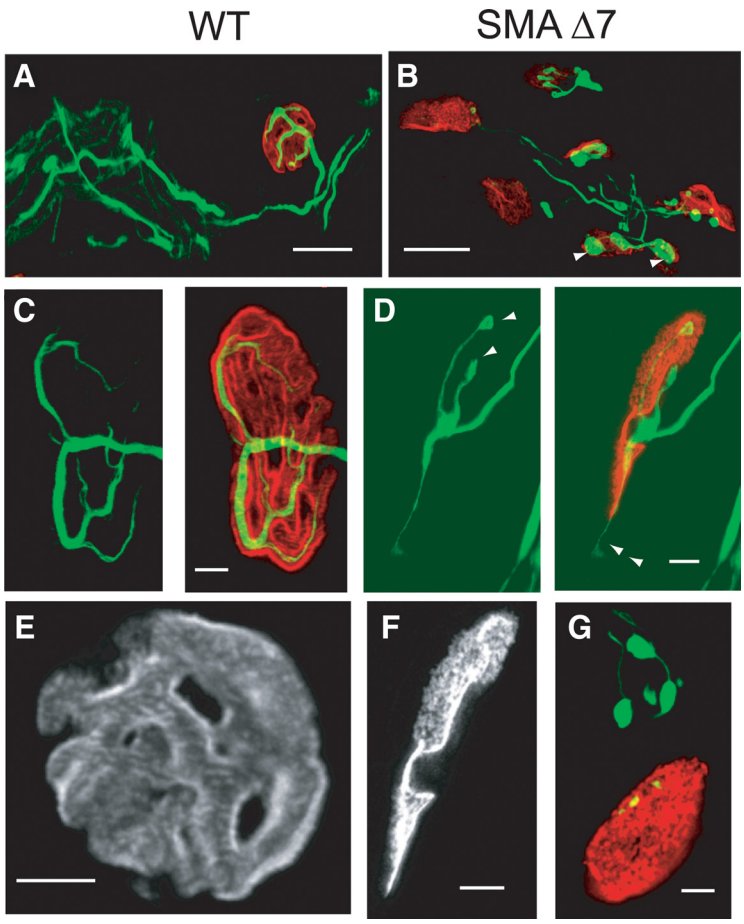

Figure 4. Innervation and morphologies of NMJs in mutant mice. ***A–G***, Immunofluorescent micrographs showing the innervation of NMJs within the TVA muscle of WT (***A***, ***C***, ***E***) and mutant (***B***, ***D***, ***F***, ***G***) mice at P15. Postsynaptic terminals were labeled with rhodamine-bungarotoxin (red) and motor neuron axons were labeled with antibodies directed against the 160 KDa chain of neurofilament (green). Scale bars: ***A***, ***B***, 20 μm; ***C–G***, 5 μm.

0.015) (Fig. 2*C*, right graph). These results show that different nerve branches within the same muscle can be functionally more affected than others by SMN deficiency.

In TVA, the mean size of the EPP in mutants was significantly reduced in comparison with wild-types (mutants: 19.1 ± 3.87; wild-types: 29.5 ± 3.22; $p < 0.022$), and the QC reduced ~55% (mutants: 5.1 ± 0.9; wild-types: 11.3 ± 1.1; $p < 0.0002$) (Fig. 2*D*, left graph). The kinetics of EPPs—mainly determined by the time course of neurotransmitter release, the passive electrical properties of the postsynaptic membrane, and the molecular characteristics of the postsynaptic receptors—was abnormally slow in the TVA (Fig. 2*D*, middle and right panels) while it was normal in the LAL (data not shown). These results are in agreement with the morphological findings (Murray et al., 2008) that TVA motor nerve terminals are impaired earlier than LAL motor nerve terminals in SMA mice. The kinetic defect detected in SMA mice is compatible with a defect on the maturation of the end plates.

Therefore, our results show that neurotransmission in the LAL muscle is relatively normal at 1 week of age, with the exception of the most caudomedial region. On the contrary, the TVA muscle-evoked neurotransmission is impaired at the same age. Our results in TVA muscle are in agreement with those recently reported for the TA muscle (Kong et al., 2009).

Progression of the neurotransmission defects

To acquire insight into the progression of the neurotransmission defect throughout the life span of SMA mice, we also studied spontaneous and evoked neurotransmission in the TVA muscle at P14–15.

At this late stage of the disease, most of the alterations observed 1 week earlier were more apparent. At 2 weeks of age, the mean size of spontaneous events (mEPPs) was approximately double in mutants (median: 2.48 mV) when compared with wild-type littermates (1.16 mV; $p < 0.001$) (Fig. 3*A*,*B*); this 100% increase contrasts with the 30% increase in mEPPs mean size observed 1 week earlier (Fig. 2*B*, left graph). The alteration in mEPPs between P7 and P14 is probably a result of the increased difference in muscle fiber size between mutant and wild types at these ages.

In contrast to the increase of the mean mEPPs size in mutants, the mean sizes of evoked release events, EPPs (Fig. 3*C*, left upper bar graph), which are due to the sum of individual mEPPs, were not significantly different between mutants (43.2 ± 9 mV) and wild-type mice (38.6 ± 4 mV). This result indicates a clear decrease in the number of vesicles fused per action potential. In fact, QC was ~50% decreased in mutants (15 ± 2.1) in comparison with wild-types (30.1 ± 4.3; $p < 0.004$) (Fig. 3*C*, right upper bar graph). Interestingly, at this age, QC in mutants was ~66% greater than a week before (Fig. 2*D*), indicating that mutant nerve terminals were still able to increase neurotransmission during this period, much like wild-types which increased their QC ~63% during this same period of time.

Normally, the kinetics of postsynaptic responses (rise and decay times of mEPPs and EPPs) become faster during the postnatal NMJ maturation period. This is due to the organization of active zones at the presynaptic terminal as well as the postsynaptic nicotinic receptors switch from the fetal subunit (γ) to the adult type (ε) receptor. However, in the SMA mutants the postsynaptic responses in the TVA muscle remained slow at 2 weeks of age and did not mature as did wild-type terminals (Fig. 3*C*, traces and lower bar graphs).

Morphological alterations in mutant nerve terminals

It has been recently shown that in SMNΔ7 SMA mutants, there is an abnormal accumulation of NF at intraterminal axonal branches, as well as a defect in the maturation of the postsynaptic terminal (Murray et al., 2008; Kariya et al., 2009; Kong et al., 2009). We have analyzed the morphological changes appearing at P15 in the contralateral TVA muscle that was studied by electrophysiology. Distal axons were visualized with antibodies against NF, and AChRs were labeled with α-bungarotoxin-rhodamine.

In wild-type littermates, NF was well distributed (Fig. 4*A*,*C*), and the postsynaptic terminal was well matured into a perforated pretzel-shaped form (Fig. 4*C*,*E*). Gutters and folds (bright and dark bands of orthogonal orientation with respect to the nerve

branches) were already evident (Fig. 4*E*). In contrast, in mutants, thin axons and NF accumulations were evident (Fig. 4*B*,*D*, arrowheads), and in some cases sprouting terminals were visualized (Fig. 4*D*, double arrowheads). At the postsynaptic site, mutants' plaques did not fully progress to the mature form but remained oval-shaped with almost no gutters and perforations. Postsynaptic receptors remained in patches, as illustrated in Figure 4, *F* and *G*. We also found denervated junctions and retracted presynaptic terminals (Fig. 4*G*). All these results showed that the maturation of the NMJ in mutants was delayed what correlates with the slowness of the end-plate potentials. It remains, however, to be determined whether all the functional changes found in mutants are solely attributed to the delay in the maturation of the NMJ, or, in addition, there are other specific alterations.

Asynchronous neurotransmitter release in nerve terminals from the LAL muscle

Subsequently, we studied the occurrence of asynchronous release, which is mainly driven by bulk Ca^{2+} accumulation during and immediately after intense stimulation (Barrett and Stevens, 1972; Atwood and Karunanithi, 2002).

In mutants, asynchronous release of neurotransmitter from nerve fibers—appearing as stochastic mEPPs in and between evoked release responses during a train of stimuli—was minimal with limited stimuli but gradually emerged during action potential long trains (Fig. 5*A*, asterisks). The occurrence of asynchronous release in mutant terminals suggested that residual Ca^{2+} accumulation was high enough to trigger this type of neurotransmitter release.

The amount of asynchronous release for a given mutant terminal, quantified as the number of mEPPs per minute during the stimulation train, was similar from trial to trial. A representative example of a terminal, challenged with three successive stimulation trains at 20 Hz, 1.5 s long, is shown in Figure 5*B*. It can be observed that the frequency of mEPPs increased linearly to approximately the same levels for all three trains, suggesting that Ca^{2+} accumulation was similar in all trials.

Next, we compared the sizes of the asynchronous release responses in mutants and wild-type littermates for different train durations. Figure 5*C* illustrates the mean frequency values from the two groups of mice (P7–8). In mutants, the frequency of asynchronous release events was greater than in wild-types, but without reaching statistical significance. This is probably due the enormous variability of the responses and the overall small impairment of the LAL nerve terminals in mutants.

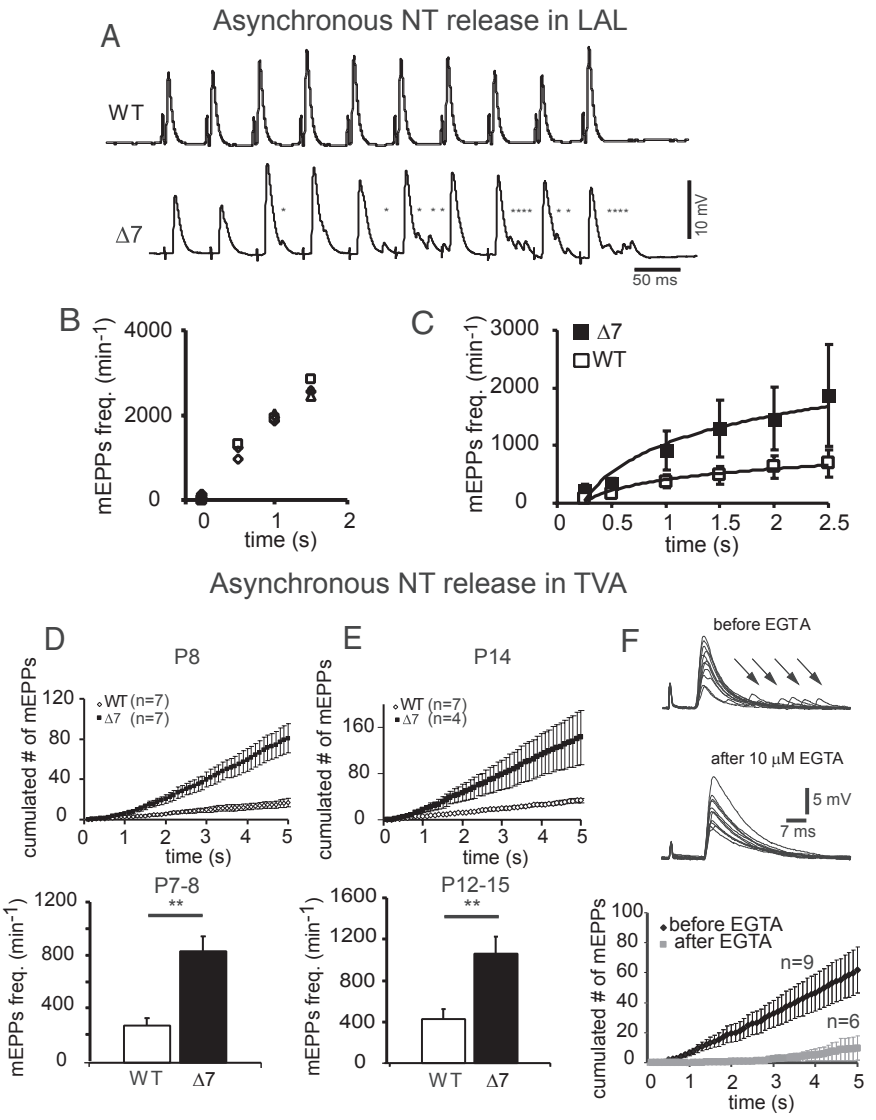

Figure 5. Asynchronous neurotransmitter release in mutant and wild-type terminals in the LAL (***A–C***, P7–8) and TVA (***D–F***, P8–15) muscles. ***A***, Representative traces of evoked end-plate potentials in response to a train of stimuli at 20 Hz from a WT and a mutant mouse. Note the appearance of asynchronous release events (asterisks) between EPPs. ***B***, Frequency of mEPPs as a function of time throughout the stimulation train (20 Hz) corresponding to three different trials in the same terminal. ***C***, Mean asynchronous mEPPs frequency in WT (open square, *n*, $N = 11, 4$) and SMA mice (black square, *n*, $N = 26, 6$). ***D***, ***E***, Graphs show mean cumulative frequency of mEPPs corresponding to asynchronous release in a WT ($n = 7$ fibers) and a mutant littermate ($n = 7$ fibers) at P8 (***D***) and P14 (***E***) during a stimulus train at 20 Hz, 5 s. ***F***, Asynchronous release (arrows in superimposed evoked traces, upper panel) disappeared in the presence of 10 μM EGTA-AM (superimposed evoked traces, lower panel) in mutants; the graph shows mean cumulative frequency of asynchronous release in mutant fibers before and after incubation with EGTA. $^{**}p < 0.005$.

Anomalous asynchronous release in nerve terminals from the TVA muscle

To verify whether the trend observed in the LAL (i.e., an apparent increased amount of asynchronous neurotransmitter release during stimulation trains in mutants) was also present in the TVA muscle, we measured asynchronous release in mutant and wild-type mice in the TVA muscle, reasoning that if synchronous release was more impaired in the TVA than in the LAL (Figs. 2, 3), it could also be true for asynchronous release.

First, we measured the cumulated number of mEPPs during a five seconds train at 20 Hz from wild-type and mutant fibers. Figure 5, *D* and *E*, shows examples of these measurements in two pair of littermates at two ages (P7–8 and P12–15, respectively). In both cases, the mean cumulated frequency was greater in mu-

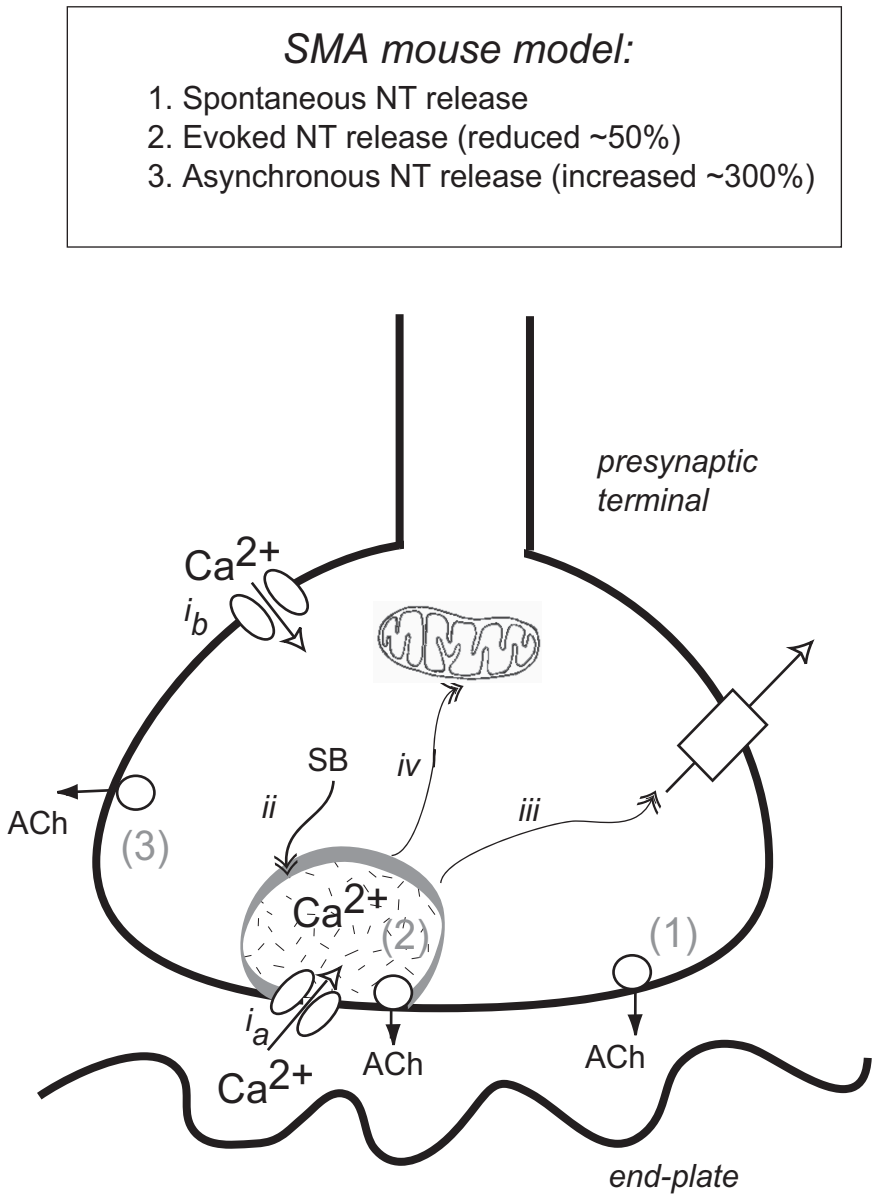

Figure 6. Modes of neurotransmitter (NT) release in nerve terminals (1–3) and proposed mechanisms for altered intraterminal Ca^{2+} homeostasis i–iv. 1, Spontaneous NT release, independent of action potential (AP) activity. 2, Synchronous NT release at nanodomains of high Ca^{2+} (shadowed area) when Ca^{2+} channels are activated by an AP (evoked release). 3, Asynchronous NT release outside active zones in response to bulk Ca^{2+} accumulation during repetitive APs firing. i, Increase of Ca^{2+} entry through Ca^{2+} channels at i_a and outside of i_b active zones. ii, Decrease of slow Ca^{2+} buffer (SB- Ca^{2+}) capacity. iii, Decrease of Ca^{2+} extrusion through Ca^{2+} pumps and/or Na^{+}-Ca^{2+} exchangers. iv, Decreased Ca^{2+} uptake by mitochondria.

tants. When we measured the cumulated mEPPs frequency at the end of the train for a number of 1-week-old mice we found that asynchronous release frequency was ~300% larger in mutants (850 ± 151 events/min) in comparison with controls (285 ± 84 events/min; $p < 0.003$). It is interesting to note that this difference persisted at 2 weeks of age with ~250% greater asynchronous release in mutants (1084 ± 176 events/min) than in controls (440 ± 97 events/min; $p < 0.003$) (n, $N = 21, 3$).

To determine whether the excess of asynchronous release we found in SMA mutants was calcium-dependent, we used the membrane-permeable slow calcium buffer EGTA-AM (10 μM) to decrease bulk Ca^{2+} concentration (Hefft and Jonas, 2005; Maximov and Südhof, 2005). Figure 5*F* shows a representative experiment of two muscular fibers recorded in the same mutant muscle one in the absence (upper trace), and the other, in the presence (lower trace) of EGTA-AM in the bath (see Materials and Methods). For clarity, evoked responses have been superimposed; note that after incubating with 10 μM EGTA-AM, asynchronous release (arrows) disappeared. The lower graph in part F of the figure illustrates the mean cumulated number of asynchronous events for mutant fibers during the stimulation trains, before (dark symbols, $n = 9$ fibers) and after EGTA (open symbols, $n = 6$ fibers) ($p < 0.015$ at 5 s). Clearly, EGTA drastically reduced asynchronous release events confirming that they were due to a high increase of intraterminal bulk Ca^{2+} in mutants during repetitive stimulation. The incubation of nerve terminals with a larger concentration of EGTA-AM (100 μM) also eliminated synchronous release (supplemental Fig. S1*C*, available at www.jneurosci.org as supplemental material).

Discussion

The mechanism(s) by which a reduction of SMN causes neurodegeneration remains unknown but, in recent years, diverse hypotheses have been postulated to explain the specific need for SMN in motor neurons, based on experimental data obtained in different animal models (McWhorter et al., 2003; Rossoll et al., 2003; Carrel et al., 2006; Jablonka et al., 2007; Oprea et al., 2008). The fact that anomalous changes in motor terminals appear earlier than motor neuron loss in the spinal cord suggests that this disease is a "dying back" process. To gain insight into the possible changes taking place in motor synapses in SMNΔ7 SMA mice, we have studied the NMJ function in two proximal muscles with electrophysiological techniques, a fast twitch (LAL) and a predominantly slow twitch (TVA) muscle. Our results show that the electrical excitability of mutant muscle fibers is preserved and that poly-innervation is functional. In addition, we found that neurotransmission in the LAL muscle is relatively normal at 1 week of age, with the exception of the most caudomedial region. On the contrary, the TVA muscle-evoked neurotransmission is clearly impaired. This functional difference correlates with similar structural findings recently reported in the same muscles in this SMA model (Murray et al., 2008). Interestingly, a previous functional study of the distal TA muscle, has found that in SMA mutants neurotransmission is decreased, and the kinetics of postsynaptic responses is slowed (Kong et al., 2009). These results are similar to what we find in the TVA, a proximal and slow twitch muscle. Comparison of data from these three muscles (LAL, TVA, and TA) is, therefore, of much interest but need to take into account that in newborn and perinatal animals the fate of the muscle fibers is changing from the embryonic to the peri-

natal and adult forms. Interestingly, in the hind-limb muscles from the SMNΔ7 SMA mouse model a delay in the maturation of the muscle fibers has been described (Kong et al., 2009). Additionally, the metabolic demands of distinct types of motor neuron (tonic versus phasic) may also be important for determining synaptic vulnerability in this disease.

The amount of neurotransmission decrease we find in mutants (~50%) does not apparently explain the paralysis observed in SMA mice. This is because this reduced amount of neurotransmitter could still produce action potentials in high input resistance atrophic muscle fibers. However, in the electrophysiological recordings, fibers with unstable membrane potential or with only-spontaneous-neurotransmitter release, which were both frequently found in mutants, were discarded, what may result in underestimation of the magnitude of the real dysfunction.

Interestingly, together with the decrease in evoked neurotransmitter synchronous release, we found an anomalous increase in asynchronous release in mutant terminals. Normally, asynchronous neurotransmitter release during intense nerve stimulation directly depends on intraterminal calcium concentration (Barrett and Stevens, 1972; Atwood and Karunanithi, 2002). We confirmed that this was also true in mutant terminals with the EGTA-AM experiments (Fig. 5*F*). Several possibilities might explain why intraterminal Ca^{2+} increases more in mutants than in control littermates during prolonged nerve stimulation (Fig. 6). These include: (1) increased Ca^{2+} entry through Ca^{2+} channels, (2) decreased slow Ca^{2+} buffer capacity, (3) decreased Ca^{2+} extrusion, and (4) decreased Ca^{2+} reuptake by intracellular organelles.

An increase in Ca^{2+} entry through Ca^{2+} channels (Fig. 6, i_a) is possible but unlikely because in mutant terminals the neurotransmitter release probability is decreased [evidenced by the greater facilitation responses during stimulation trains, see supplemental Figure S1*A*,*B*, available at www.jneurosci.org as supplemental material, and also the study by Kong et al. (2009)], which is exactly the opposite of what is expected if there is more Ca^{2+} influx through Ca^{2+} channels coupled to release sites (Thomson, 2000). Moreover, motor neurons in culture from Smn deficient mice have been demonstrated to exhibit a reduced integration of the $Ca_v2.2$ Ca^{2+} channels into axonal growth cones (Jablonka et al., 2007). Nevertheless, an aberrant activation of Ca^{2+} channels outside the release sites, such as $Ca_v1.1$-4 Ca^{2+} channels (Fig. 6, i_b) is plausible. However, this activity normally takes place before the establishment of the synapse and disappears when the nerve terminal makes contact with the muscle (Chow and Poo, 1985; Hata et al., 2007).

The second possibility, a decrease in slow Ca^{2+} buffering capacity (Fig. 6, ii), is feasible. We found prolonged EPPs and mEPPs decays in the TVA mutant fibers (Figs. 2*B*,*D*, 3*C*), and similar results have been obtained measuring the postsynaptic currents (EPCs) in the TA muscle (Kong et al., 2009), as expected if Ca^{2+} concentration at the entry sites remained high for a longer period of time. However, the same trait can be observed if there is retardation in the switching from embryonic to adult AChRs, as the open times are longer in the embryonic channel than in the adult form of the receptor, which has been demonstrated to occur in SMNΔ7 SMA mutant mice (Kong et al., 2009).

A defect of Ca^{2+} extrusion, due to a primary defect of the Ca^{2+}-pumps or on the Na^+-Ca^{2+} exchanger (Fig. 6, iii), which is the third possibility, is hardly probable, as asynchronous release after the stimulation train decreased in mutants as fast as in controls (supplemental Fig. S1*D*, available at www.jneurosci.org as supplemental material), suggesting that after the entry of Ca^{2+} has ended, the pumps and the Na^+-Ca^{2+} exchanger restored the Ca^{2+} basal levels within a normal time span. Finally, the forth possibility, a decreased Ca^{2+} reuptake by intracellular organelles, such the mitochondria (Fig. 6, iv), is feasible. Mitochondria sequestration of Ca^{2+} during moderate-to large stimulation is especially relevant in nerve terminals. Mitochondria dysfunction has been proven in distinct motor neuron diseases, including amyotrophic lateral sclerosis (Hervias et al., 2006; Nguyen et al., 2006), and spinal and bulbar muscular atrophy (Ranganathan et al., 2009). In SMA patients, alteration on mitochondria function in muscles has been reported (Gobernado et al., 1980; Sperl et al., 1997; Berger et al., 2003). It is, however, controversial whether SMA is a primary mitochondriopathy. It might be that, in muscles, the mitochondria defects result from the atrophy of the muscle. Nevertheless, to our knowledge, no study has been performed on nerve terminal mitochondria in SMA human patients. In the SMNΔ7 SMA mouse model, it has been reported that presynaptic mitochondria in the diaphragm are smaller than in wild-type littermates, while no differences were found at the postsynaptic sites (Kariya et al., 2008). Another study, in the same mouse model, found a decrease in the number of mitochondria in the presynaptic terminals of the TA muscle (Kong et al., 2009). Furthermore, a mitochondrial dysfunction has been reported to exist, when SMN is knocked down in cultured neuronal cells, in particular there is a decrease on ATP levels and an increase of free radicals in Smn siRNA knock-down neurons (Acsadi et al., 2009). A reduction of Ca^{2+} uptake by the mitochondria would increase cytosolic Ca^{2+}, which will interfere with the normal buffering of the Ca^{2+} load during intense stimulation in nerve terminals (Friel and Tsien, 1994).

Further studies are required to determine which of the proposed mechanism(s) is responsible for the altered intraterminal Ca^{2+} homeostasis in SMNΔ7 SMA mutants, and how this alteration could participate in the actual degeneration process. Further work in this direction might help understand the pathogenesis of this disease, and therefore, to increase our options for meaningful therapeutic intervention.

References

Acsadi G, Lee I, Li X, Khaidakov M, Pecinova A, Parker GC, Hüttemann M (2009) Mitochondrial dysfunction in a neural cell model of spinal muscular atrophy. J Neurosci Res 87:2748–2756.

Atwood HL, Karunanithi S (2002) Diversification of synaptic strength: presynaptic elements. Nat Rev Neurosci 3:497–516.

Barrett EF, Stevens CF (1972) The kinetics of transmitter release at the frog neuromuscular junction. J Physiol 227:691–708.

Berger A, Mayr JA, Meierhofer D, Fötschl U, Bittner R, Budka H, Grethen C, Huemer M, Kofler B, Sperl W (2003) Severe depletion of mitochondrial DNA in spinal muscular atrophy. Acta Neuropathol 105:245–251.

Butchbach ME, Edwards JD, Schussler KR, Burghes AH (2007) A novel method for oral delivery of drug compounds to the neonatal SMNDelta7 mouse model of spinal muscular atrophy. J Neurosci Methods 161:285–290.

Carrel TL, McWhorter ML, Workman E, Zhang H, Wolstencroft EC, Lorson C, Bassell GJ, Burghes AH, Beattie CE (2006) Survival motor neuron function in motor axons is independent of functions required for small nuclear ribonucleoprotein biogenesis. J Neurosci 26:11014–11022.

Chow I, Poo MM (1985) Release of acetylcholine from embryonic neurons upon contact with muscle cell. J Neurosci 5:1076–1082.

Cifuentes-Diaz C, Nicole S, Velasco ME, Borra-Cebrian C, Panozzo C, Frugier T, Millet G, Roblot N, Joshi V, Melki J (2002) Neurofilament accumulation at the motor endplate and lack of axonal sprouting in a spinal muscular atrophy mouse model. Hum Mol Genet 11:1439–1447.

Colman H, Nabekura J, Lichtman JW (1997) Alterations in synaptic strength preceding axon withdrawal. Science 275:356–361.

Crawford TO, Pardo CA (1996) The neurobiology of childhood spinal muscular atrophy. Neurobiol Dis 3:97–110.

Fischer U, Liu Q, Dreyfuss G (1997) The SMN-SIP1 complex has an essential role in spliceosomal snRNP biogenesis. Cell 90:1023–1029.

Friel DD, Tsien RW (1994) An FCCP-sensitive Ca^{2+} store in bullfrog sympathetic neurons and its participation in stimulus-evoked changes in $[Ca^{2+}]$i. J Neurosci 14:4007–4024.

Gennarelli M, Lucarelli M, Capon F, Pizzuti A, Merlini L, Angelini C, Novelli G, Dallapiccola B (1995) Survival motor neuron gene transcript analysis in muscles from spinal muscular atrophy patients. Biochem Biophys Res Commun 213:342–348.

Gobernado JM, Gosalvez M, Cortina C, Lousa M, Riva C, Gimeno A (1980) Mitochondrial functions in chronic spinal muscular atrophy. J Neurol Neurosurg Psychiatry 43:546–549.

Hata K, Polo-Parada L, Landmesser LT (2007) Selective targeting of different neural cell adhesion molecule isoforms during motoneuron myotube synapse formation in culture and the switch from an immature to mature form of synaptic vesicle cycling. J Neurosci 27:14481–14493.

Hefft S, Jonas P (2005) Asynchronous GABA release generates long-lasting inhibition at a hippocampal interneuron-principal neuron synapse. Nat Neurosci 8:1319–1328.

Hervias I, Beal MF, Manfredi G (2006) Mitochondrial dysfunction and amyotrophic lateral sclerosis. Muscle Nerve 33:598–608.

Jablonka S, Beck M, Lechner BD, Mayer C, Sendtner M (2007) Defective Ca^{2+} channel clustering in axon terminals disturbs excitability in motoneurons in spinal muscular atrophy. J Cell Biol 179:139–149.

Kariya S, Park GH, Maeno-Hikichi Y, Leykekhman O, Lutz C, Arkovitz MS, Landmesser LT, Monani UR (2008) Reduced SMN protein impairs maturation of the neuromuscular junctions in mouse models of spinal muscular atrophy. Hum Mol Genet 17:2552–2569.

Kariya S, Mauricio R, Dai Y, Monani UR (2009) The neuroprotective factor Wld(s) fails to mitigate distal axonal and neuromuscular junction (NMJ) defects in mouse models of spinal muscular atrophy. Neurosci Lett 449:246–251.

Kong L, Wang X, Choe DW, Polley M, Burnett BG, Bosch-Marcé M, Griffin JW, Rich MM, Sumner CJ (2009) Impaired synaptic vesicle release and immaturity of neuromuscular junctions in spinal muscular atrophy mice. J Neurosci 29:842–851.

Le TT, Pham LT, Butchbach ME, Zhang HL, Monani UR, Coovert DD, Gavrilina TO, Xing L, Bassell GJ, Burghes AH (2005) SMNDelta7, the major product of the centromeric survival motor neuron (SMN2) gene, extends survival in mice with spinal muscular atrophy and associates with full-length SMN. Hum Mol Genet 14:845–857.

Lefebvre S, Bürglen L, Reboullet S, Clermont O, Burlet P, Viollet L, Benichou B, Cruaud C, Millasseau P, Zeviani M, et al (1995) Identification and characterization of a spinal muscular atrophy-determining gene. Cell 80:155–165.

Liu Q, Fischer U, Wang F, Dreyfuss G (1997) The spinal muscular atrophy disease gene product, SMN, and its associated protein SIP1 are in a complex with spliceosomal snRNP proteins. Cell 90:1013–1021.

Lorson CL, Hahnen E, Androphy EJ, Wirth B (1999) A single nucleotide in the SMN gene regulates splicing and is responsible for spinal muscular atrophy. Proc Natl Acad Sci U S A 96:6307–6311.

Martin AR (1955) A further study of the statistical composition on the end-plate potential. J Physiol 130:114–122.

Maximov A, Südhof TC (2005) Autonomous function of synaptotagmin 1 in triggering synchronous release independent of asynchronous release. Neuron 48:547–554.

McWhorter ML, Monani UR, Burghes AH, Beattie CE (2003) Knockdown of the survival motor neuron (Smn) protein in zebrafish causes defects in motor axon outgrowth and pathfinding. J Cell Biol 162:919–931.

Meister G, Bühler D, Pillai R, Lottspeich F, Fischer U (2001) A multiprotein complex mediates the ATP-dependent assembly of spliceosomal U snRNPs. Nature cell biology 3:945–949.

Monani UR, Lorson CL, Parsons DW, Prior TW, Androphy EJ, Burghes AH, McPherson JD (1999) A single nucleotide difference that alters splicing patterns distinguishes the SMA gene SMN1 from the copy gene SMN2. Hum Mol Genet 8:1177–1183.

Monani UR, Sendtner M, Coovert DD, Parsons DW, Andreassi C, Le TT, Jablonka S, Schrank B, Rossol W, Prior TW, Morris GE, Burghes AH (2000) The human centromeric survival motor neuron gene (SMN2) rescues embryonic lethality in Smn(−/−) mice and results in a mouse with spinal muscular atrophy. Hum Mol Genet 9:333–339.

Murray LM, Comley LH, Thomson D, Parkinson N, Talbot K, Gillingwater TH (2008) Selective vulnerability of motor neurons and dissociation of pre- and post-synaptic pathology at the neuromuscular junction in mouse models of spinal muscular atrophy. Hum Mol Genet 17:949–962.

Nguyen DM, Yeow WS, Ziauddin MF, Baras A, Tsai W, Reddy RM, Chua A, Cole GW Jr, Schrump DS (2006) The essential role of the mitochondria-dependent death-signaling cascade in chemotherapy-induced potentiation of Apo2L/TRAIL cytotoxicity in cultured thoracic cancer cells: amplified caspase 8 is indispensable for combination-mediated massive cell death. Cancer J 12:257–273.

Oprea GE, Kröber S, McWhorter ML, Rossoll W, Müller S, Krawczak M, Bassell GJ, Beattie CE, Wirth B (2008) Plastin 3 is a protective modifier of autosomal recessive spinal muscular atrophy. Science 320:524–527.

Pellizzoni L, Yong J, Dreyfuss G (2002) Essential role for the SMN complex in the specificity of snRNP assembly. Science 298:1775–1779.

Ranganathan S, Harmison GG, Meyertholen K, Pennuto M, Burnett BG, Fischbeck KH (2009) Mitochondrial abnormalities in spinal and bulbar muscular atrophy. Hum Mol Genet 18:27–42.

Redfern PA (1970) Neuromuscular transmission in new-born rats. J Physiol 209:701–709.

Rossoll W, Jablonka S, Andreassi C, Kröning AK, Karle K, Monani UR, Sendtner M (2003) Smn, the spinal muscular atrophy-determining gene product, modulates axon growth and localization of beta-actin mRNA in growth cones of motoneurons. J Cell Biol 163:801–812.

Ruiz R, Casañas JJ, Südhof TC, Tabares L (2008) Cysteine string protein-alpha is essential for the high calcium sensitivity of exocytosis in a vertebrate synapse. Eur J Neurosci 27:3118–3131.

Sanes JR, Lichtman JW (1999) Development of the vertebrate neuromuscular junction. Annu Rev Neurosci 22:389–442.

Santafé MM, Garcia N, Lanuza MA, Uchitel OD, Tomás J (2001) Calcium channels coupled to neurotransmitter release at dually innervated neuromuscular junctions in the newborn rat. Neuroscience 102:697–708.

Sperl W, Skladal D, Gnaiger E, Wyss M, Mayr U, Hager J, Gellerich FN (1997) High resolution respirometry of permeabilized skeletal muscle fibers in the diagnosis of neuromuscular disorders. Mol Cell Biochem 174:71–78.

Thomson AM (2000) Facilitation, augmentation and potentiation at central synapses. Trends Neurosci 23:305–312.